ISSN 0006-3509, Biophysics, 2018, Vol. 63, No. 5, pp. 779–790. © Pleiades Publishing, Inc., 2018.
Original Russian Text © A.G. Lastovetsky, E.N. Minina, 2018, published in Biofizika, 2018, Vol. 63, No. 5, pp. 975–988.

COMPLEX SYSTEMS BIOPHYSICS

A Triangulation Approach to Checking the Reliability of Estimation of Oscillatory Modes Embedded in an ECG Signal

A. G. Lastovetsky[a], * and E. N. Minina[b], **

[a]*Central Research Institute of Health Care Organization and Informatization, Ministry of Health of the Russian Federation Moscow, 127254 Russia*

[b]*Taurid Academy, Vernadsky Crimean Federal University, Simferopol, 295007 Russia*

**e-mail: albertlast@yandex.ru*

***e-mail: cere-el@yandex.ru*

Received April 11, 2018; in final form, August 9, 2018

Abstract—It is important to perform an analytical study of the oscillatory modes embedded in an ECG signal on individuals in certain occupations (power station operators, pilots, military officers, drivers, sportspeople, etc.) and those who experience pronounced emotional stress while carrying out important work. Reliability of studying the oscillatory modes was achieved by using and comparing several methods (triangulation), thus allowing evaluation of the results obtained by studying spatio-temporal variances, the ordered vs. stochastic character, and the periodic vs. stochastic character of the dynamics of an ECG signal. The oscillatory modes of the ECG signal structure were studied in various conditions using graphic illustrations obtained by converting the ECG signal in the phase plane. The orderliness, periodicity, and stochastic features of a time series of R–R intervals were examined using the entropy-dynamic approach and the phase-plane and phase-curve methodologies. Nonlinear phenomena were qualitatively described using the elementary part of the theory of catastrophes. Dysfunctional and pathological conditions were associated with either a significant expansion of the phase graph (PG) shape with significant variations in amplitude and time parameters and an increase in the degree of chaos or a distinct periodicity with a loss of variability, a decrease in the chaotic component, and a mathematical degeneration of the cycle. The results of the ECG-based entropy analysis and its PG were quantitatively comparable with data obtained by a rheographic recording of the biological signal; this finding supporting the reliability of the results. Constructing a phase curve using a nonparametric method helped us to detect hidden functional features of the cardiodynamics system. This study substantially contributes to the development of preventive methods based on testing cardiac activity in the primary medical and social care system.

Keywords: triangulation, ECG signal, oscillatory mode

DOI: 10.1134/S0006350918050147

INTRODUCTION

The majority of physiological oscillations are not strictly periodic; rhythms change irregularly with time not only in response to external factors and noise disturbances [1–3], but also as a result of their fractal nature. As an example, nonlinear changes arise in the heart rhythm because the heart function is affected by various factors, including neurohumoral mechanisms of higher autonomic centers. Methods to analyze heart rate variability in terms of time are the simplest and the most common and are well understood. However, when studying oscillatory processes, it is important to distinguish the variability of time-related periodic components of stationary function modes and oscillatory processes with chaotic components, which are characteristic of transition states and are time independent. The analysis is further complicated by the fact that a nonlinear character of oscillations is impossible to describe using common statistical methods [2–4].

Nonlinear methods are thought to provide promising tools to evaluate the variances of amplitude and time variables of depolarization and repolarization. However, evaluation of oscillatory modes embedded in a myocardial signal has not been standardized for use in physiological and clinical studies; such studies have a limited potential and are mostly of theoretical interest [2, 3, 5]. The objective of this work was to provide an analysis of the oscillatory modes in an ECG signal with the use of various methods, data sets, and theoretical concepts.

Abbreviations: ECG, electrocardiogram; PG, phase graph; MSD, mean square deviation; VO_{2max}, maximal oxygen consumption.

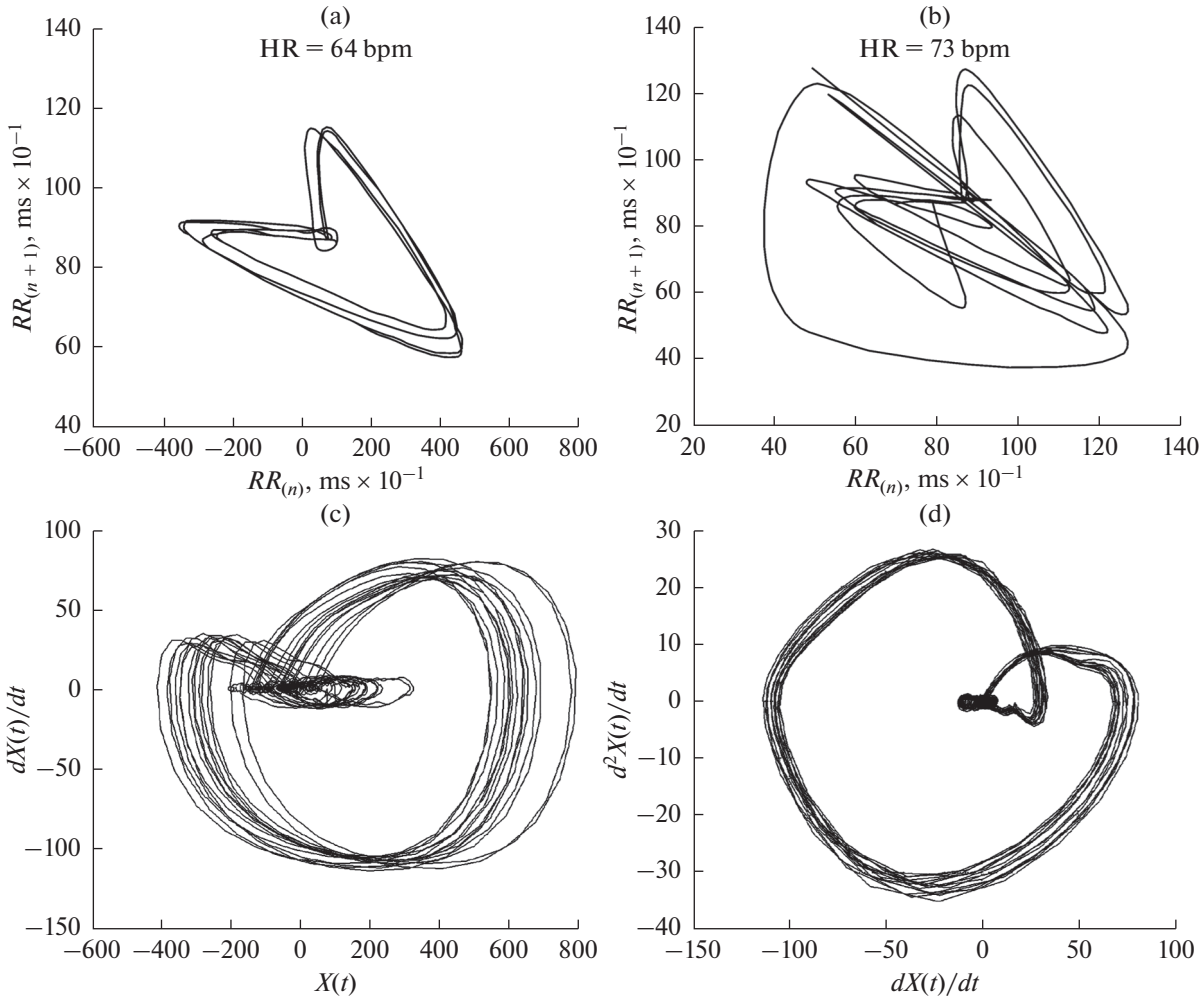

Fig. 1. Maps of the ECG signal in a phase space based on the data (a, b) [7] and (c, d) [8].

MATERIALS AND METHODS

Evaluation of oscillatory modes by phase graph (PG) elements. To evaluate the heterogeneity of electrogenesis exemplified by repolarization of the ventricular myocardium, inclusion of both the total variance of repolarization and its spatial direction and time interval in the analysis are recommended [6]. It is possible to carry out such an analysis noninvasively with a method that describes a dynamic system in a phase space of states and is broadly used in physics and applied mathematics. Several approaches to constructing a PG have been described in the literature, including a time-delay method and a method to estimate the first derivative (or the rate of change) for the variable in question (Fig. 1). The resulting phase portraits of the ECG signal are comparable and distinctly similar in shape. However, the portraits are based on limited data, thus rendering it unfeasible to statistically verify the phase mapping of the ECG signal and to provide a physiological grounding.

A large data set ($n = 8600$) was used to study the PG parameters. An analysis and the information significance of the PG parameters have been described previously [9–15]. We found that the parameters reflect the electrophysiological and metabolic features of the myocardial function and can provide prognostic markers to evaluate the risk of cardiac and hemodynamic pathologies.

The PG of a single-lead ECG was based on the ideas of cognitive computer graphics and automated image recognition and was constructed in the coordinates $z(t)$, $\dot{z}(t)$, where $\dot{z}(t)$ is the rate of change in the electrical activity of the heart at the time point t. The rate was determined using the FAZAGRAF software and hardware complex, which utilizes an original information technology designed to process the ECG signal in the phase space.

Although an ECG (Fig. 2a) is not a periodic function of time, trajectories of individual cycles (Fig. 2b) occur in a certain local region of the phase plane $z(t)$,

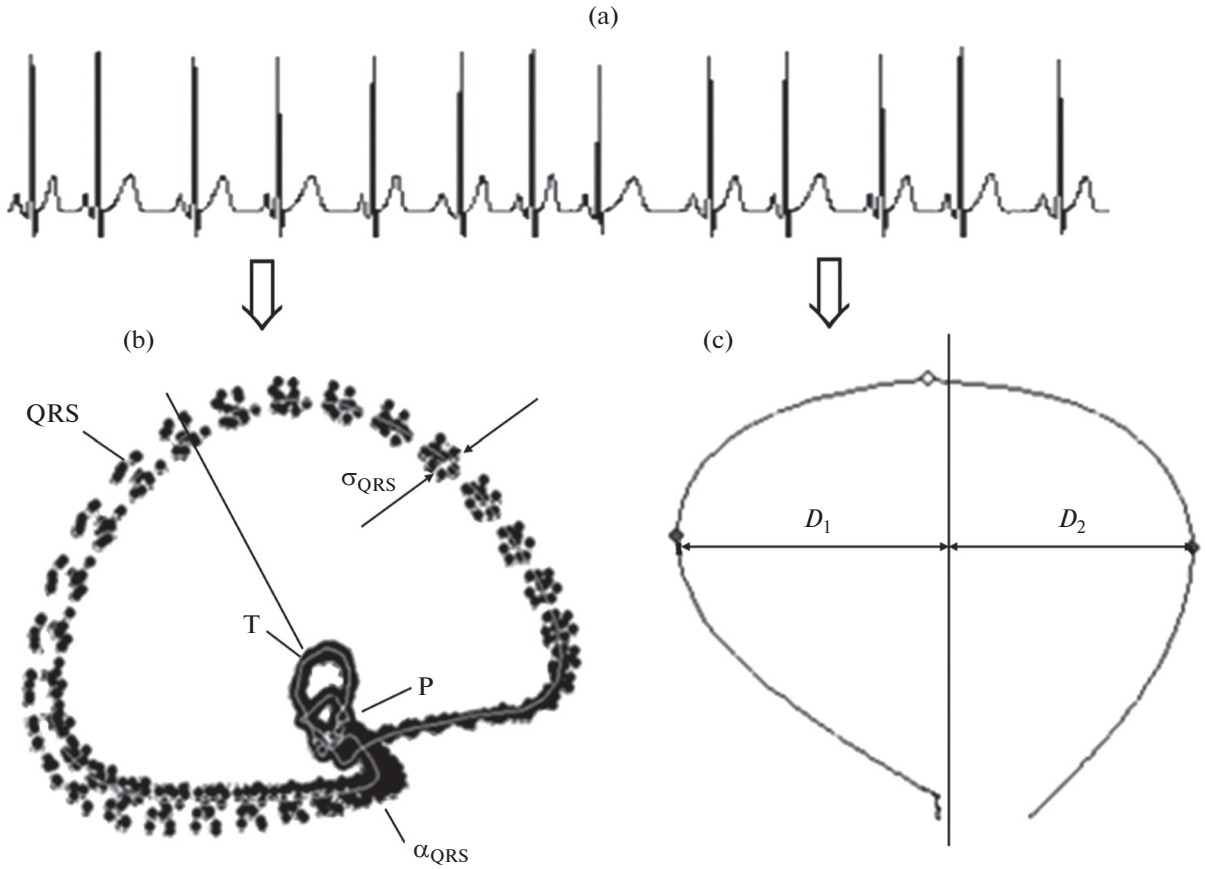

Fig. 2. Steps of ECG processing: (a) initial ECG; (b) its phase trajectory, or a PG; (c) a PG region corresponding to the T-wave of a single-lead ECG and the method to assess its symmetry, which was determined as D_1/D_2.

$\dot{z}(t)$ in the majority of cases; the region is an attractor in the form of a limiting cycle.

One feature of the method is that the Hausdorff distances between all pairs of the phase trajectories Q_n and Q_m of individual ECG cycles are used to select the atypical ECG cycles (extrasystoles and artifacts) and to evaluate the averaged phase trajectory (Fig. 2c):

$$R_H(Q_n, Q_m) = \max\left\{\max_{q_n \in Q_n} \min_{q_m \in Q_m} \rho(q_n, q_m), \max_{q_m \in Q_m} \min_{q_n \in Q_n} \rho(q_n, q_m)\right\},$$

where $\rho(q_n, q_m) = \|q_n - q_m\|$ is the Euclidean distance between the points (normalized vectors) $q_n = (z_n, \dot{z}_n) \in Q_n$ and $q_m = (z_m, \dot{z}_m) \in Q_m$, which lie in the phase plane.

To study the oscillatory modes of the ECG signal in various conditions using the PG of the ECG signal in the phase plane, we examined the following parameters: PG variance (σ, units), T-wave symmetry (β_T, units), and mean square deviation (MSD) of T-wave symmetry (β_T MSD, units).

Entropy dynamics modeling used to study the oscillatory modes in the time series of R–R intervals in the ECG signal. To evaluate the ordered vs. chaotic character, variability of the time series of R–R intervals was studied in terms of entropy [16–18].

The mathematical methods that are used to assess the degree of chaos in dynamic series utilize the following well-known equation for entropy:

$$H = -\sum_{i=1}^{n} p_i \log_2 p_i, \quad (1)$$

which Shannon introduced to assess the level of uncertainty for a system that occurs in one of its n states with the probability p_i, $i = 1, \ldots, n$.

The higher H is, the farther the system is from its ordered state. The maximal Shannon entropy is reached when $p_i = 1/n$, that is, the states of the system are equally possible. It follows that the entropy (1) takes values in a range of $[0, \log_2 n]$.

To calculate the degree of chaos for a dynamic series on the basis of entropy, we considered separate regions of the series of discrete signal values. A time series of N discrete values was divided into M consecutive fragments (windows) and the relative increase in entropy was calculated for each of the windows:

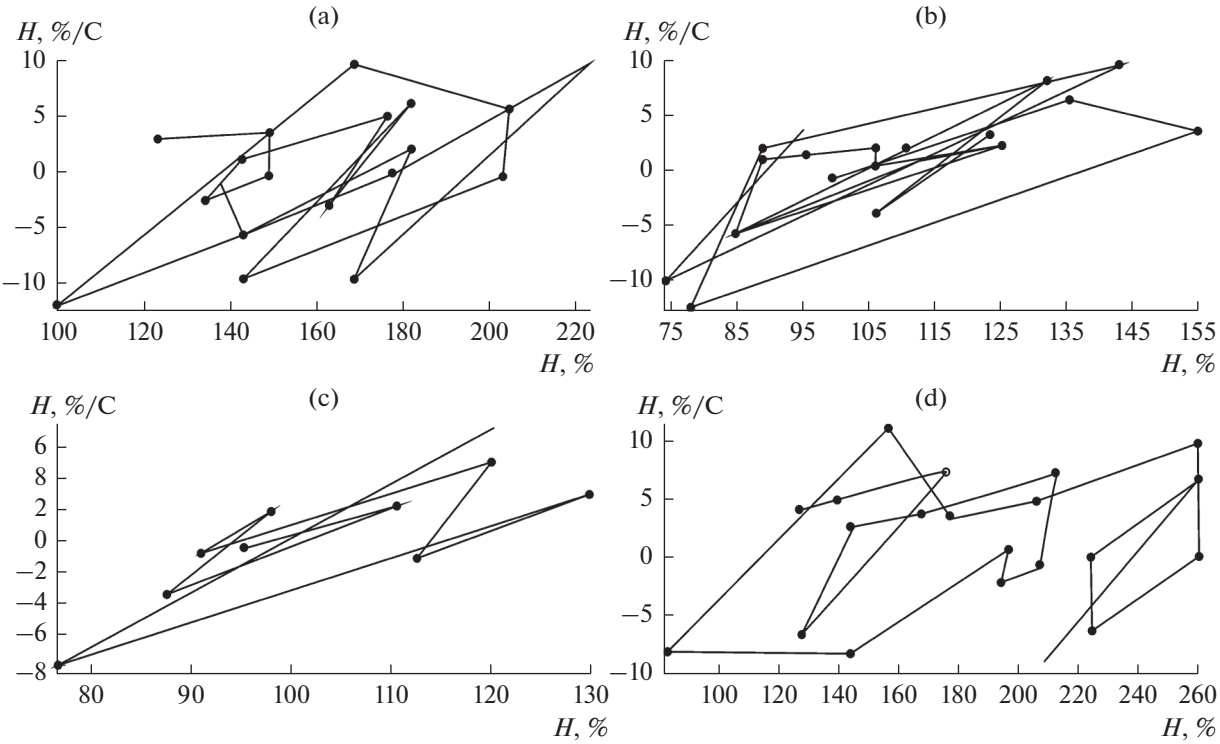

Fig. 3. Entropy PG variants obtained for individuals of different cohorts: (a, b) 15-year-old athletes at the peak of competition (fatigue), (c) a 47-year-old female, and (d) an 8-year-old child in emotional stress.

$$H_l = \frac{-\sum_{j=1}^{n} p_{jl} \log p_{jl}}{H_1} \cdot 100\%, \quad l = 1,\ldots, M, \qquad (2)$$

where p_{jl} is the frequency at which the time series values observed in the lth fragment occur in the jth fragment ($j = 1, \ldots, n$) of values defined by the threshold δ and

$$H_1 = -\sum_{j=1}^{n} p_{j1} \log_2 p_{j1} \qquad (3)$$

is the entropy calculated for the first (reference) window.

We have previously demonstrated that substantially different entropy phase maps (Fig. 3) are obtained for time series of R–R intervals, while time-related variability parameters are much the same (a heart rate of 69–72 bpm, IN 67–75 units).

The entropy of the R–R time series were studied using ECG signals recorded in various conditions with an electrocardiograph and a rheoplethysmograph.

The phase-plane technique used to study the oscillatory modes in the time series of R–R intervals in the ECG signal. A series of R–R intervals in the ECG signal is generated by a complex nonlinear system, which is difficult to describe with a differential equation. However, the character of its behavior remains the same at all scales. Studies of complex systems have shown that a system audit is the most informative when entropy parameters of a system are examined together with its phase characteristics. The approach makes it possible to rank the system states and evolutionary trends.

In this study, the peripheral capillary blood flow was measured by finger photoplethysmography (with a Pal'tsevoi Fotopletizmograph instrument) and the results were automatically processed by special software to obtain the normalized entropy E:

$$E_i = -\frac{\sum_{k=1}^{N} p_k \log p_k}{E_1} \cdot 100\%, \qquad (4)$$

where i is the index (the ordinal number of the measurement; $i = 1, 2, 3, \ldots, N$), p_k is the probability that the instantaneous frequency falls within the kth partition interval of the width Δ (Δ = 50 ms), and $E_1 = -\sum_{k=1}^{N} p_k \log p_k$ is the entropy of the first (reference) measurement.

An entropy PG of the time series of R–R intervals was constructed automatically and stored in the software interface; its parameters were evaluated graphically.

A mathematical method based on the catastrophe theory in the analysis of the ECG signal dynamics.

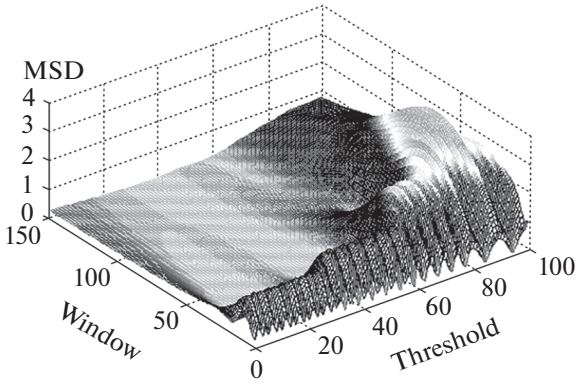

Fig. 4. The nonlinear dependences of dynamic variables of entropy oscillations in three-dimensional space; a fold is a feature.

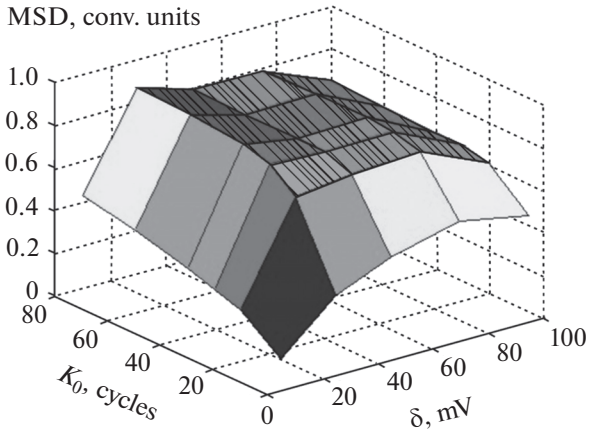

Fig. 5. MSD of entropy changes between an athlete and a nonathlete as a function of the window width K_0 and the insensitivity threshold δ. The area of acceptable values of K_0 and δ is crosshatched.

Nonlinear phenomena are possible to describe based on the elementary part of the catastrophe theory (Fig. 4).

It is clear that the shape of the entropy change plot $H(i)$ depends on the parameters used in Eq. (2) to determine $H(i)$, that is, on the window width K_0 and the threshold insensitivity δ to changes in values of the dynamic series under study. We selected the "optimal" values for K_0 and δ of Eq. (2). Because formal methods to determine the optimal values of K_0 and δ do not yet exist, their values were selected experimentally based on a pragmatic criterion, which was the maximum mean-square deviation (MSD) of entropy changes in individuals from cohorts that differed in adaptation potential. A series of computational experiments was performed with different values of K_0 and δ for the purpose and the value of the function $\Psi(K_0, \delta)$ was evaluated for each pair of K_0 and δ values as MSD of the entropies $H_1(i)$ and $H_2(i)$ obtained for an athlete and a nonathlete, respectively.

$$\Psi(K_0, \delta) = \frac{1}{N}\sum_{i=1}^{N}[H_1(i) - H_2(i)]^2. \quad (5)$$

Figure 5 shows a plot of the function $\Psi(K_0, \delta)$ with acceptable values of the K_0 and δ parameters. At these values, the entropy deviations of an athlete and a nonathlete are the greatest (MSD > 0.6) and vary within a broad range:

$$K_0 > 10 \text{ cycles}, \quad (6)$$

$$20 < \delta < 80 \text{ ms}. \quad (7)$$

The phase-curve method used to evaluate the periodicity vs. chaotic character of a time series of R–R intervals of the ECG signal. Entropy periodograms of time series of R–R intervals were additionally analyzed for several young male groups that differed in the organization of the cardiohemodynamic system. Original software employed the nonparametric Abbe–Laffler–Kinman method, wherein phase-curve quality depends on the distance between the points that are closest in phase and folding is performed by frequencies rather than by periods. A phase curve can be examined visually with a plot to determine the period and structure and to qualitatively evaluate them according to the algorithm below.

For the time series $\{t_k, y_k\}$, $k = 0, 1, ..., N-1$, which must not be evenly spaced and includes N observations of the process $y(t)$, the phase was calculated for each time point t_k at a preset exploratory period $P = \nu^{-1}$:

$$x_k = \text{frac}\left(\frac{t_k - t^*}{P}\right), \quad (8)$$

where P is the period, t_k is the observation time point, and t^* is an arbitrary time point.

The phases X_k were arranged in the order of increasing value, and the ordered values were designated $X_{[k]}$, so that

$$0 \le x_{[0]} \le x_{[1]} \le ... \le x_{[N-1]} < 1. \quad (9)$$

Then,

$$\vec{y}_k \equiv y(x_{[k]}) \quad (10)$$

are observations of the series that correspond to Eq. (9) and are consecutive on a phase diagram rather than on a time axis. Parameter (11) showed how ordered points were on the phase curve. When consecutive points are close to each other on average, s^2_{in} is low; when points are chaotically distributed, s^2_{in} is of the same order of magnitude as the total variance of the series (12):

$$s^2_{\text{in}} = \frac{1}{1(N-1)}\sum_{k=0}^{N-2}(\vec{y}_{k+1} - \vec{y}_k)^2, \quad (11)$$

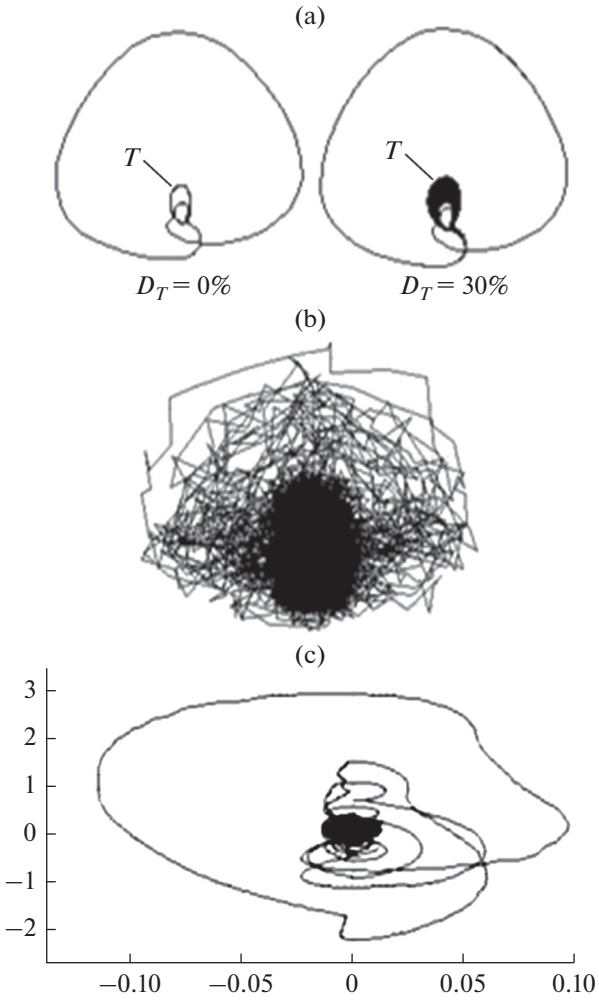

Fig. 6. PG examples. (a) Model experiments were performed using different values for the variance of amplitude and temporal parameters of the T-wave. (b) The PG of the ECG at a high level of internal and external perturbations. (c) A PG observed in a patient 1 day before a fatal outcome.

$$s^2 = \frac{1}{N-1}\sum_{k=0}^{N-1}(y_k - \bar{y})^2. \quad (12)$$

It should be expected that the ratio is far lower than unity when the exploratory period is close to the actual period P_0 and that $\Theta \sim 1$ at other frequencies. The resulting equation is the Abbe–Lafler–Kinman criterion:

$$\Theta_N(v) = \frac{\sum_{k=0}^{N-2}(\vec{y}_{k+1} - \vec{y}_k)^2}{2\sum_{k=0}^{N-1}(y_k - \bar{y})^2}. \quad (13)$$

We examined 120 males of two age groups that differed in adaptation potential. A homogeneous group of young males (18–19 years of age) was divided into two subgroups, cohort A of 30 males who were not regularly involved in sports and cohort B of 30 high-ranking athletes (football players and boxers) with a training history of at least 6 years.

Cohort C included 20 healthy middle-aged males (40–45 years) with low-level locomotor activity. Cohort D included 40 healthy males involved in regular exercise. The cohort D males were boxers that differed in training history: 20 were neophyte boxers with a history of less than 5 years; the others were veteran boxers with a training history of at least 10 years.

Physical working capacity (PWC) was measured in a two-step test on a VE-02 bicycle ergometer. We determined the PWC-170 and calculated aerobic parameters, including both absolute values and values normalized to body weight (maximal oxygen consumption (VO_{2max}, L/min; and VO_{2max}/kg, mL/min/kg), which provided integral markers of the functional potential of the cardiorespiratory system. In addition, we used tests with physical loading increased in a stepwise manner and vestibular loading (Voyachek's test in the Barany chair). A Spiro spirograph was used to measure the minute ventilation V_E (L); a KP-01 gas analyzer served to measure the carbon dioxide production, V_{CO_2}. The CO_2 ventilation equivalent VE_{CO_2} (units) was calculated as V_E/V_{CO_2} (units), reflecting the minute ventilation necessary to produce 1 L of CO_2. The respiratory compensation point, which characterizes the transition to mostly anaerobic energy production and reflects the ventilation threshold of anaerobic supply, was determined from the ventilator equivalent dynamics as the moment when ventilation increases dramatically relative to V_{CO_2}.

The results were statistically analyzed using the STATISTICA 6.0 package (StatSoft, United States). Deviations of parameter distributions were evaluated via the Kolmogorov–Smirnov test. Differences in parameters between the states before and after exercise or an increase in external loading were tested for significance by the nonparametric Wilcoxon *T*-test. The parametric Student *t*-test was used in the case of a normal distribution.

RESULTS

At the first step of the study, PG parameters were analyzed to evaluate the oscillations of T-wave parameters; the results demonstrated reliably that an increase in their variance in consecutive cardiac cycles increased the PG scatter. In particular, an increase in the variance D_T of the amplitude and temporal parameters that characterize the T-wave shape led to a greater scatter of points in the corresponding loop of the PG (Fig. 6a).

We observed that dysfunctions and pathological conditions were associated with either a substantial

Table 1. The dynamics of T-wave symmetry in various conditions in boxers who differ in their training level

Conditions	Experienced ($n = 20$)	Neophyte ($n = 20$)	Significance
Rest	0.68 ± 0.01	0.74 ± 0.02	<0.05
Vestibular loading after rest	0.66 ± 0.01	0.76 ± 0.01	<0.001
Peak loading	0.95 ± 0.02	1.20 ± 0.02	<0.001
After exercise	0.86 ± 0.03	1.00 ± 0.01	<0.001
Vestibular loading in fatigued state	0.79 ± 0.01	1.10 ± 0.02	<0.001
Recovery, 6 min	0.69 ± 0.02	0.97 ± 0.01	<0.001
Recovery, 15 min	0.66 ± 0.01	0.87 ± 0.02	<0.001

expansion of the PG shape with substantial variations in amplitude and temporal parameters and an increase in the degree of chaos (Fig. 6b) or a distinct periodicity with a loss of variability, a decrease in the chaotic component, and a degeneration of the cycle (Fig. 6c). PG parameters describe the oscillatory processes of electrogenesis. As an example, the shape of the T-wave in the phase space, that is, the degree of its symmetry from one cycle to another reflects the quality of depolarization and repolarization oscillations. The T-wave shape is known to depend on the duration and magnitude of transmembrane action potentials in various regions of the myocardium. The dynamics of T-wave symmetry (β_T, units) in response to an increase in external loading had its characteristics in athletes who were of the same age but differed in training history and functional reserve level (Table 1).

It is noteworthy that alternation of ECG elements and, in particular, that of T-wave shape with changes in T-wave symmetry in consecutive cycles led to a characteristic PG splitting, which additionally characterized the oscillatory mode of the biological signal. As an example, the increase in β_T MSD in neophyte boxers was, on average, 20.5% higher than in experienced boxers ($p < 0.05$).

Like the extent of chaos in the state of a thermodynamic system, any physical factor is characterized by an extension of the phase portrait and an increase in its effective volume with the scatter σ. The PG characterized the chaotic component in the mechanisms of heart activity and provided further information to understand whether the regulation of its functional state was optimal. As an example, successful adaptation corresponded to a certain scatter range of phase trajectories of the ECG signal in healthy young males aged 18–19 years; the range was 19.3 ± 1.0 units on average. The parameter σ decreased to 14.6 units with the increasing sport level.

The scatter σ increased by more than 60% after the respiratory compensation point in the athletes, suggesting a broad range of systemic modifications for the regulation of the cardiovascular system. In contrast, only a minor increase in PG scatter was observed in the young males with lower reserve parameters (Fig. 7). Changes in PG scatter were indicative of how efficiently the system switches the regulatory modes and reflects the transition to a new dynamic state with another level of homeokinesis. The quality of oscillatory modes should also be classed with adaptation and sanogenesis reserves, representing a resource that accumulates as a result of systematic specific exercise associated with sports.

In spite of the high correlation between β_T MSD and σ ($r = 0.78$, $p < 0.001$), the parameters revealed certain differences in the mechanisms that regulating the oscillatory process. As an example, β_T MSD increased by 18.5% on average ($p < 0.05$) on vestibular loading regardless of the training level, while σ remained constant. In contrast, both of the parameters increased significantly during physical loading.

The extent of T-wave symmetry or variance of the T-wave shape, as well as changes in dimensions, in a PG characterized the oscillatory modes of electrogenesis and reflected various components of its regulation. A quantitative determination of possible oscillatory modes might solve the paradox of linear relation-

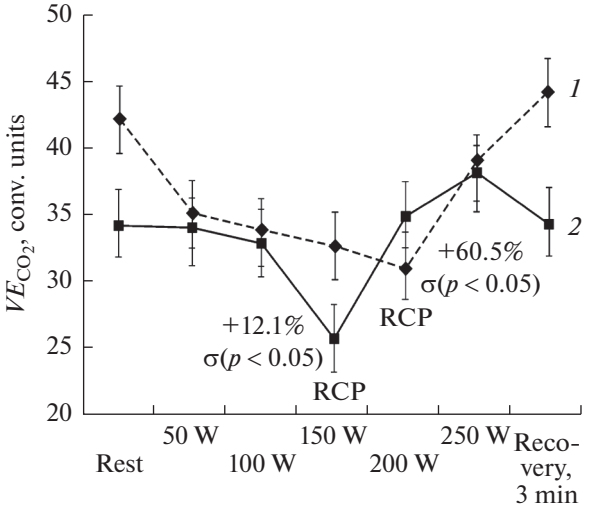

Fig. 7. The dynamics of VE_{CO_2} in (*1*) athletes and (*2*) nonathletes aged 19–20 years during a test with increasing physical power loading and recovery. RCP, respiratory compensation point.

Table 2. Changes in parameters that characterize the systemic response of cardiohemodynamics to an increase in external loading in groups of subjects who differed in adaptation potential

Subject group	Parameter/conditions			
	σ, units		*H*, %	
	rest	loading	rest	loading
Cohort A	17.3 ± 2.0	25.0 ± 1.3*	93.3 ± 5.9	160.3 ± 19.5***
Cohort B	14.6 ± 0.5	32.2 ± 1.5**	75.8 ± 3.2	110.6 ± 9.2***

Differences were significant at * $p < 0.05$, ** $p < 0.01$, or *** $p < 0.001$.

ships between the parameters to ensure homeostasis in favor of an increase in the formation of levels of the homeokinesis regulation to switch the functioning rate as in a technical instrument.

At the second step of the study, the entropy dynamics approach was used to evaluate the oscillatory modes of the ECG signal.

The systemic organization of cardiodynamics was studied in two cohorts of young males who differed in training level. VO_{2max} in young males of cohort B were 33.3% higher than in males of cohort A ($p < 0.001$). Relative VO_{2max} reached 50.1 ± 1.1 mL/min/kg in cohort B and did not exceed 36 mL/min/kg in cohort A. In a stepwise loading test, the dynamics of parameters of the cardiovascular system in the athletes indicated that the system functioned economically and efficiently.

The level of information and energy resources in the form of its orderliness and/or self-organization during switching of regulatory modes makes it necessary to evaluate this adaptation reserve. Table 2 summarizes the changes in parameters that were obtained to characterize the systemic response of hemodynamics to an increase in external loading in subject groups that differed in adaptation potential. Different methods were used and compared with the analysis of periodic and nonperiodic components in entropy periodograms of R–R intervals. It should be noted that the characteristics of the entropy of R–R intervals and its changes reflected the quality of the organization of the cardiohemodynamic system and its regulatory reserves. As is known, any system has a certain organization level that is called critical. When the system organization is below the critical level, ordering processes and, possibly, self-organization prevail in the system. When the actual level is higher than critical, disorganization processes prevail. At the critical level, which is sometimes called the entropy balance level, ordering and disorganization processes are balanced, and the system assumes a steady state [18]. The extent of the balance was studied at the next step of our work.

At the third step, the oscillatory modes of a time series of R–R intervals of the ECG signal were studied in the phase plane. Entropy oscillations suggest an alternation of self-organization and disorganization periods, that is, increases in orderliness alternate with increases in disorderliness. The entropy change ΔE assumed both negative and positive values (the entropy E is always positive, as is evident from the compensatory minus sign in Shannon's equation). Shapovalov [18, 19] was the first to theoretically demonstrate the possibility of entropy oscillations. Such oscillations were believed to be basically impossible because they contradict Prigogine's theorem of minimal entropy production. The theorem states that the second derivative of entropy with respect to time cannot change its sign in the vicinity of a steady state. However, mathematically, equations that describe oscillations must include an alternating derivative of at least order two. Second- and higher-order derivatives of entropy have been shown to change in sign when the system is affected by an entrostat. An entrostat is defined as a system whose entropy changes are possible to neglect in comparison with entropy changes of the system of interest [19]. In our study, young males (18–19 years) who differed in adaptation potential displayed significant differences in mean entropy H, its variation range ΔH, and the variation range $\Delta H'$ of its rate of change in the observation period in the phase plane; the signal was detected by rheography (Table 3). In the second subgroup, which included young males with a higher adaptation potential, the entropy was lower by 50.0% ($p < 0.001$), the entropy variation range was half as high on average ($p < 0.001$), and the variation range of entropy rate of change was 44.8% lower ($p < 0.05$) than in young males of the first subgroup. When the same parameters were compared in middle-aged males (40–45 years of age), the phase-plane analysis similarly showed significant differences in the entropy variation range ΔH and the range of the rate of change of the entropy $\Delta H'$, while the mean entropy H did not significantly differ between the subgroups (Table 4).

It should be concluded that the cardiohemodynamics system functions far more strenuously to maintain homeostasis and the adaptation cost is higher in the subgroups with a lower training level and, therefore, a lower adaptation potential. It may be possible to use this finding as an early prognostic sign of dysfunction.

Entropy periodograms of time series of R–R intervals were additionally analyzed in the same young

Table 3. Changes in parameters of the entropy phase portrait of a time series of R–R intervals in the subgroups of young males (18–19 years of age) who differed in adaptation potential

Subject subgroup	Parameter		
	H, %	ΔH, %	$\Delta H'$, %/C
Cohort A	110.3 ± 3.9	62.2 ± 4.1	4.3 ± 0.3
Cohort B	77.2 ± 2.2	22.5 ± 3.2	2.5 ± 0.5
Significance of difference	$p < 0.001$	$p < 0.001$	$p < 0.05$

Table 4. Changes in the parameters of the entropy phase portrait of a time series of R–R intervals in the subgroups of males aged 40–45 years who differed in adaptation potential

Subject subgroup	Parameter		
	H, %	ΔH, %	$\Delta H'$, %/C
Cohort C	114.4 ± 8.1	70.2 ± 8.3	10.4 ± 0.9
Cohort D	98.3 ± 4.1	45.9 ± 6.4	7.5 ± 1.1
The significance of the difference	–	$p < 0.05$	$p < 0.05$

males of cohorts A and B, but using the ECG signal (Fig. 8). The results were quantitatively comparable with the results obtained using the rheographic signal, supporting the reliability of the findings.

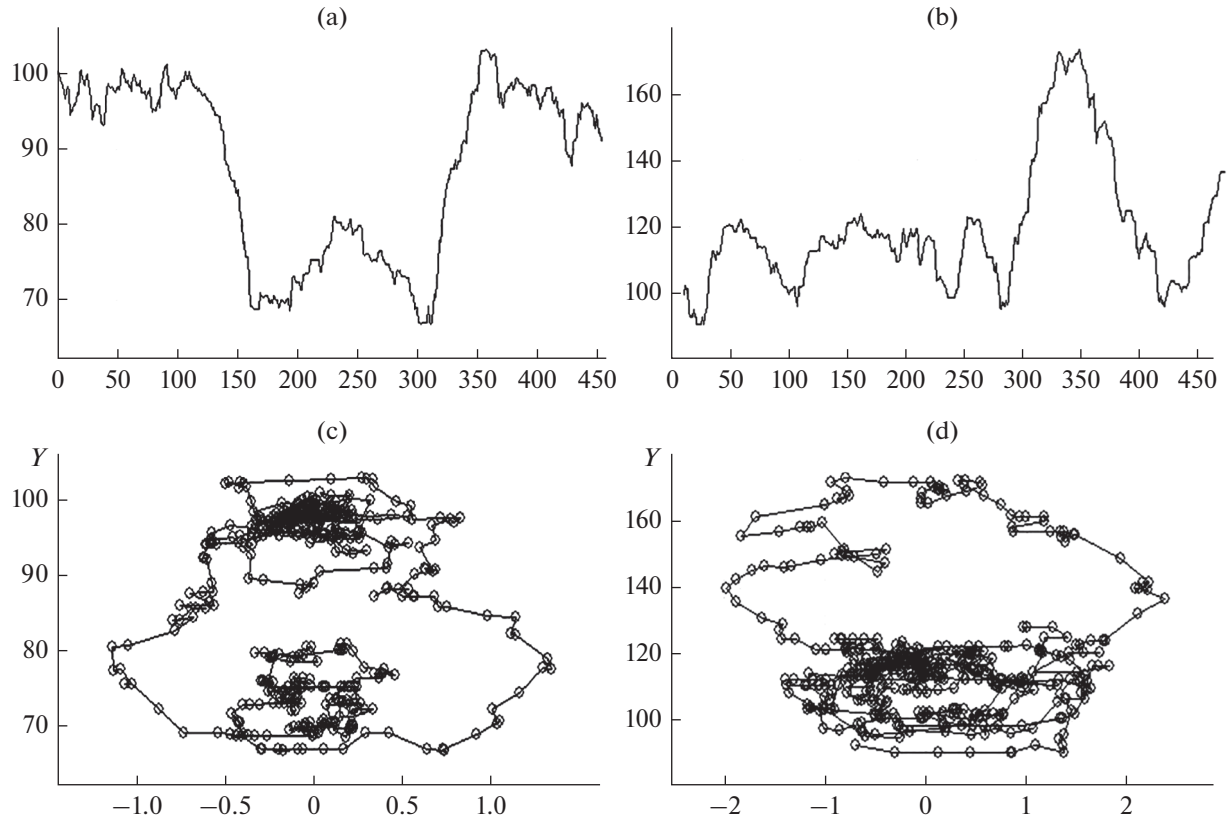

Fig. 8. (a, b) Entropy oscillations and (c, d) entropy PGs of a time series of R–R intervals of the ECG signal in (a, c) a 19-year-old athlete and (b, d) a 43-year-old male with a lower adaptation potential.

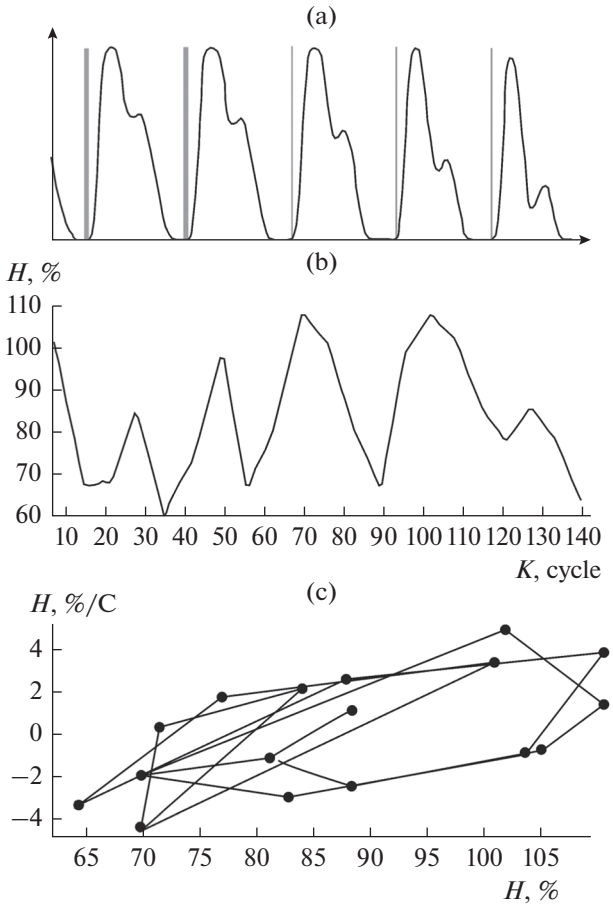

Fig. 9. The characteristics of a time series of R–R intervals in individuals with an optimal regulatory status and sufficient reserves of cardiohemodynamis: (a) a rheogram fragment (heart rate 76 bpm), (b) dynamics of entropy of the time series (a window of ten beats), and (c) PG of entropy.

At the fourth step, the phase-curve method was used to evaluate the periodicity vs. chaotic character of the entropy of a time series of R–R intervals of the ECG signal; the results were compared with earlier findings.

When the regulation of a system is in a normal balanced state, the following periodogram is presumably observed and reflects the specifics of the temporal systemic organization (Fig. 9). As is seen from Fig. 10, cryptic temporal features of the systemic organization can be detected using the Abbe–Lafler–Kinman method to analyze the periodogram and constructing a phase-curve. If we disregard the theoretical periodogram "curve," which consists of "point–point" groups, then points of entropy change values seem stochastic. However, a conversion to a phase-curve reveals cryptic regular periodicity (Fig. 10). Certain issues were observed in the periodogram characteristics of individuals with a lower adaptation potential (Fig. 11). As is seen from Fig. 11, the entropy PG was asymmetric relative to the horizontal axis and was

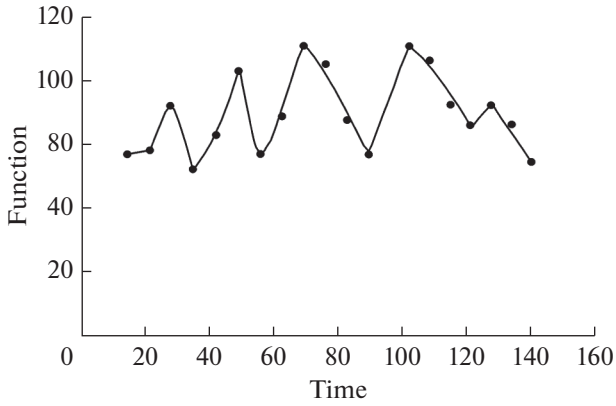

Fig. 10. The phase curve of the periodogram of a time series of R–R intervals with optimal reserves.

broader, reflecting an inadequate character of system rearrangement during adaptation; a greater range of entropy variation suggested a substantial cost of adaptation. The analysis can be expanded to include the phase-curve of the periodogram (Fig. 12).

A further qualitative analysis was performed in the young male cohorts that differed in functional potential; it showed that the phase curve of the entropy periodogram had a distinct temporal organization in 78.2% of the subjects in the cohort with a high adaptation potential. In contrast, qualitative temporal organization was not observed for the phase-curve of the entropy periodogram in the cohort with a lower adaptation potential and a less "trained" cardiohemodynamics system. The phase-curve method used to additionally analyze the entropy periodogram of R–R intervals made it possible to observe cryptic features of the temporal systemic organization of cardiohemodynamics and to identify prognostic signs by analyzing the system state vector [20]. Thus, several different methods were used to increase the reliability of studying the oscillatory modes in the ECG signal, as is characteristic of a triangulation approach (Fig. 13).

CONCLUSIONS

(1) The significance of studying the oscillatory modes in ECG signals was achieved by using and comparing different methods (triangulation), making it possible to evaluate the results obtained by studying the spatiotemporal variances, the ordered vs. stochastic character, and the periodic vs. stochastic character of the dynamics of the ECG signal.

(2) Oscillatory processes of electrogenesis are described by PG parameters. Dysfunctions and pathological conditions are associated with either a substantial expansion of the PG shape with substantial variations in amplitude and temporal parameters and an increase in the degree of chaos or a distinct periodicity with a loss of variability, a decrease in the chaotic

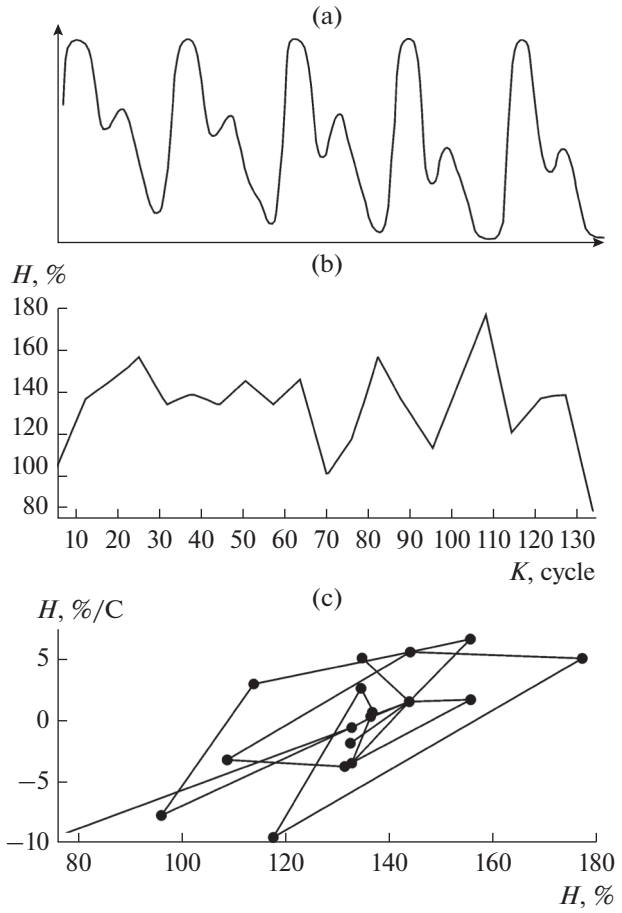

Fig. 11. The characteristics of a time series of R–R intervals in individuals with lower reserves of cardiohemodynamis: (a) a rheogram fragment (heart rate 75 bpm), (b) dynamics of entropy of the time series (a window of en beats), and (c) PG of entropy.

component, and a mathematical degeneration of the cycle.

(3) Alternation of ECG elements and, in particular, that of T-wave shape with changes in T-wave symmetry in consecutive cycles led to a characteristic PG splitting, which additionally characterized the oscillatory mode of the biological signal.

(4) The increase in β_T MSD in neophyte boxers was 20.5% higher than in experienced boxers ($p < 0.05$).

(5) Changes in PG scatter were indicative of how efficiently the system switches the regulatory modes and reflects the transition to a new dynamic state with another level of homeokinesis.

(6) The extent of T-wave symmetry or variance of T-wave shape, as well as changes in dimensions, in a PG characterized the oscillatory modes of electrogenesis and reflected various components of its regulation.

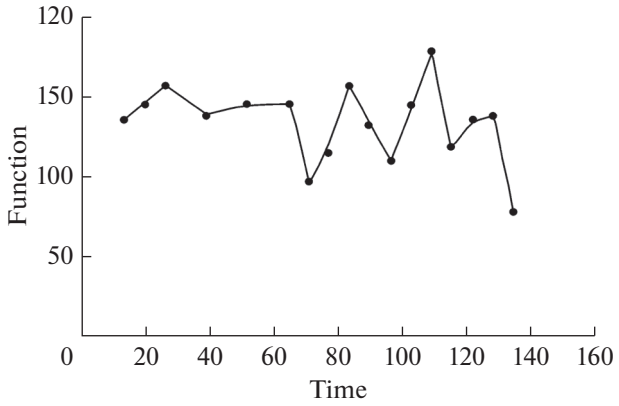

Fig. 12. The phase curve of the periodogram of a time series of R–R intervals with lower reserves.

(7) Characteristics of R–R interval entropy and its changes are indicative of the adaptation potential of the function of the cardiohemodynamics system.

(8) In young males with a higher adaptation potential, the entropy was lower by 50.0% ($p < 0.001$), the entropy variation range was half as high on average ($p < 0.001$), and the variation range of the entropy rate of change was 44.8% lower ($p < 0.05$) than in young males of the first subgroup. When the same parameters were compared in middle-aged males (40–45 years of age), significant differences were similarly observed in entropy variation range ΔH and the range of the entropy rate of change $\Delta H'$, while the mean entropy H did not significantly differ between the subgroups.

(9) The results of the ECG-based entropy analysis and its PG were quantitatively comparable with data obtained by a rheographic recording of the biological signal; the finding support the reliability of the results.

(10) A phase curve constructed by the Abbe–Lafler–Kinman nonparametric method helped to detect the cryptic adaptive possibilities of the cardiohemody-

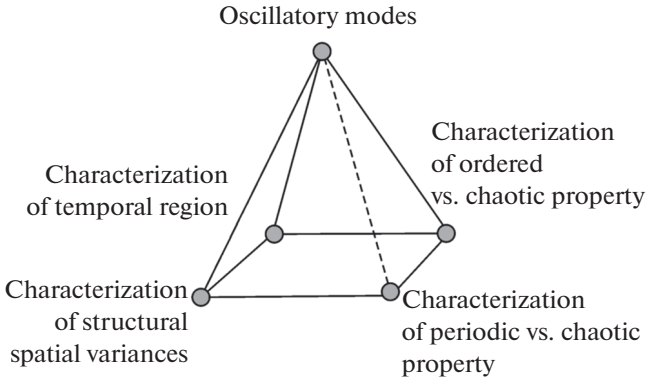

Fig. 13. The scheme of triangulation in studying the oscillatory modes of the ECG signal.

namics system. The phase-curve of the entropy periodogram had a distinct temporal organization in 78.2% of the subjects in the cohort with a high adaptation potential. In contrast, a qualitative temporal organization was not observed for the phase curve of the entropy periodogram in the cohort with a lower adaptation potential and a less "trained" cardiohemodynamics system.

(11) This study substantially contributes to the development of preventive methods of cardiac activity testing in the primary medical and social care system.

REFERENCES

1. L. Glass, Nature **410**, 277 (2001).
2. L. V. Mezentseva, Biophysics (Moscow) **56** (3), 510 (2011).
3. L. V. Mezentseva, Biophysics (Moscow) **59** (1), 119 (2014).
4. O. L. Bokeriya and M. B. Biniashvili, Ann. Aritmol. **10** (2), 79 (2013).
5. P. S. Chan, J. Amer. Coll. Cardiol. **48**, 112 (2006).
6. N. V. Arteyeva and J. E. Azarov, Ann. Noninvasive Electrocardiol. **22** (1), 12360 (2017).
7. L. V. Mezentseva, S. S. Pertsov, F. Yu. Kopilov, and A. G. Lastovetsky, Biophysics (Moscow) **62** (3), 499 (2017).
8. O. A. Voloshina, V. P. Oleinik, S. N. Kulish, and Al Otti Sami, Radioelectr. Komp'yut. Sist., No. 4 (45), 29 (2010).
9. E. N. Minina and L. S. Fainzilberg, Vestn. Nov. Med. Tekhnol. **21** (3), 22 (2014).
10. E. N. Minina, Vestn. Nov. Med. Tekhnol. **8** (1), 1-8 (2014).
11. E. N. Minina, Khimiya **1** (67) (4), 26 (2015)
12. E. N. Minina, Uch. Zap. Tavrich. Nats. Univ. im. V. I. Vernadskogo, Ser. Biol. Khim. **26**(65) (2), 148 (2013)
13. L. S. Fainzilberg and E. N. Minina, Klin. Inform. Telemed. **9** (10), 33 (2013)
14. L. S. Fainzilberg and E. N. Minina, Kibernet. Vychisl. Tekh., No. 1, 5 (2014)
15. E. N. Minina and L. S. Fainzilberg, Ross. Kardiol. Zh. **12** (128), 7 (2015).
16. A. A. Yashin, *Living Matter* (LKI, Moscow, 2010) [in Russian].
17. Yu. L. Klimontovich, Usp. Fiz. Nauk **158** (1), 59 (1989).
18. V. I. Shapovalov and N. V. Kazakov, Nat. Sci. **6** (7), 467 (2014).
19. V. I. Shapovalov, Int. J. Appl. Math. Stat. **26** (16), (2012).
20. E. N. Minina and A. G. Lastovetskii, Vestn. Nov. Med. Tekhnol. **12** (2), 2–1, (2018).

Translated by T. Tkacheva